Theoretical study of the deexcitation of C_2 in collisions with helium

J.M. Robbe, H. Lavendy, D. Lemoine, and B. Pouilly

Laboratoire de Spectroscopie Moléculaire, URA 779 du CNRS, Université de Lille Flandres Artois, F-59655 Villeneuve d'Ascq Cedex, France

Abstract. Rotational deexcitation cross-sections are calculated for C_2 ground state in collisions with He in an IOS treatment after the relevant ab initio potential surfaces have been determined. The corresponding rate constants are then determined for temperatures relevant to interstellar clouds.

Key words: collisions – interstellar matter – configuration interaction

1. Introduction

There has been considerable interest in the C_2 molecule since his discovery in interstellar molecular clouds (Souza & Lutz 1977). Of particular importance for the thermal balance of interstellar medium is the determination of rotational deexcitation of C_2 in collisions with He or molecular hydrogen H_2, species which are abundant in interstellar clouds. Recently, we have presented Infinite-Order-Sudden (IOS) calculations of rotational deexcitation of C_2 in collisions with H_2 based on ab initio electronic potential curves (Lavendy et al. 1991). In the present article, we shall extend our calculations to the C_2–He system. The quantum method for the calculation of the intermolecular potential surface which will be presented in Sect. 2 is an extension of the method presented earlier for the C_2–H_2 and H_2–H_2 systems (Lavendy et al. 1987, 1991). In Sect. 3 we shall present the results of IOS calculations of the cross-sections for rotational deexcitation of C_2. We shall also compare the rate constants with the corresponding ones in the C_2–H_2 system and we shall discuss the results in view of the electronic potential surfaces involved in the inelastic transfer processes.

2. Interaction energy and potential surface

The quantum technique for calculation of energy surfaces of Van der Waals systems has been presented in detail elsewhere. Only the relevant features will be summarized here. We will assume that the C_2 molecule remains in its $X^1\Sigma^+$ ground state with an internuclear separation fixed at the equilibrium value $r_e = 2.35$ bohr.

2.1. Atomic and molecular orbital bases

The basis set of gaussian functions must be large enough to give a reliable description of each isolated partner and to allow the deformation of the electronic cloud of one partner in the presence

of the other. We use for the C atoms the $(11\,s, 7\,p)$ gaussian basis set of Huzinaga & Sakai (1969) contracted to $(6\,s, 4\,p)$. Two d orbitals (with exponents equal to 0.70 and 0.29) are added on each C atom to allow the correct correlation of the π molecular shell. For He, we use the $7\,s$ gaussian basis of Huzinaga (1965) contracted to $4\,s$ and augmented by one diffuse s orbital (0.059), four p orbitals (1.20, 0.4, 0.13, 0.06) and one d function (0.25), as suggested by Miller and co-workers (1988) in their He–N_2^+ potential surface calculations. These diffuse functions allow a correct description of polarisation and dispersion effects.

The interaction energy is the sum of intravalence shell correlation, polarisation and dispersion energies. To calculate the intra-valence shell correlation of C_2, we start from the self-consistent field (SCF) occupied orbitals of the ground state completed by optimised virtual orbitals which are determined by means of the polarised atomic orbitals (PAO) technique (Chambaud et al. 1984). To take into account polarisation and dispersion effects, we add a second shell of virtual orbitals obtained from the distortion of the SCF occupied orbitals when a charge is placed in a direction parallel or perpendicular to the internuclear axis. For the He atom, we use natural orbitals (two s and one p) resulting from a full configuration interaction (CI) calculation of the ground state, as was done in our previous study of C–He (1991).

2.2. Configuration interaction space

To calculate the interaction energy of the supersystem C_2–He, individual molecular orbital sets are orthogonalized for each geometry. This technique induces a non-symmetrical deformation of the molecular orbitals of the isolated systems, which is compensated by specific excitations in the CI process. Most of the correlation energy is given by monoexcitations and diexcitations from the two dominant configurations $(\sigma_g^2 \sigma_u^2 \sigma_g^2 \sigma_u^2 \pi_u^4\ 1s^2$ and $\sigma_g^2 \sigma_u^2 \sigma_g^2 \sigma_g^2 \pi_u^4\ 1s^2)$. These diexcitations contribute to part of the dispersion energy, but most of the effect comes from simultaneous monoexcitations on each partner. Lastly polarisation effects are described by monoexcitations into the second shell of orbitals.

The interaction energy is given by:

$$E_{int}(R) = E_{C_2-He}(R) - E_{C_2-He}(\infty) - E_{BSSE},$$

where R is the distance between the center of mass of C_2 and He and E_{BSSE} is the basis set superposition error, calculated with the counterpoise method of Boys & Bernardi (1970).
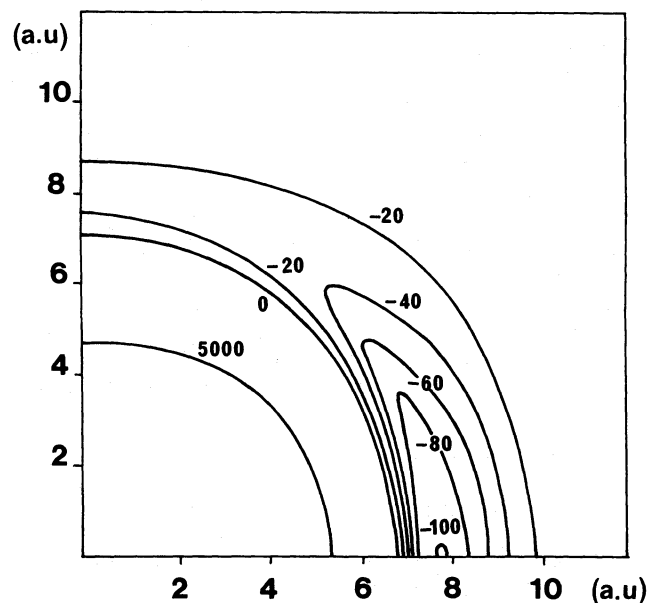
2.3. Results

The interaction energy of C_2–He is calculated for intermolecular separations ranging from 3.0 to 12.0 bohr and for seven orienta-

680

Table 1. Interaction energies[a] for six selected geometries of the C_2–He system

R(bohr)	θ=0°	θ=15°	θ=30°	θ=45°	θ=60°	θ=75°	θ=90°
3.0	249348	240565	220069	180061	138290	111824	103042
4.0	67123	63184	52266	38760	27537	20797	18611
5.0	11363	10638	8770	6486	4585	3409	3033
5.5	4093	3851	3227	2429	1721	1285	1149
6.0	1269	1217	1058	816	583	441	397
6.5	289	280	265	220	160	120	109
7.0	-23	-16	5	14	15	10	8
7.5	-95	-85	-63	-38	-26	-22	-20
8.0	-99	-87	-65	-42	-30	-26	-24
8.5	-77	-69	-51	-34	-25	-23	-22
9.0	-52	-46	-37	-28	-21	-19	-19
10.0	-17	-17	-17	-16	-15	-10	-10
12.0	-3	-3	-4	-5	-4	-3	-2
30.0	0	0	0	0	0	0	0

[a] units are in 10^{-6} au

Fig. 1. Contour plot of the C_2–He potential energy surface (μH)

tion angles (θ) between the internuclear axis of the C_2 molecule and the atomic partner. The results are displayed in Table 1 and a contour plot of the C_2–He potential energy surface is given in Fig. 1. We observe that the minimum of the potential surface corresponds to a linear approach ($\theta = 0$) as observed in the C_2–H_2 calculation by Lavendy et al. (1991).

3. IOS cross-sections calculations

In the standard close-coupling (Dickinson 1979, Arthurs & Dalgarno 1960, Secrest 1975) treatment of the collision dynamics the total wave function is expanded in terms of $|jlJM\rangle$ asymptotic wave functions obtained by vector-coupling the $|lm_l\rangle$ wave

function which describes the relative orbital motion of the two collision partners and the $|jm_j\rangle$ state which describes the rotational states of the C_2 molecule, namely

$$\Psi(R,r) = \sum_{jlJM} \frac{1}{R} C_{jl}^{JM}(R) \, |jlJM\rangle. \tag{1}$$

Here, j, l and J denote respectively the total angular momentum of the isolated C_2 molecule, the orbital angular momentum of the two partners, and the total angular momentum of the C_2–He system. M, m_j, and m_l are the projections of J, j, and l, respectively, along the space-fixed Z axis. The expansion coefficients in Eq. (1) satisfy the usual close-coupled (CC) equations which are diagonal in the total angular momentum J and in its projection M on the space-fixed Z axis.

In the infinite-order-sudden (IOS) approximation, (Dickinson 1979, Secrest 1975, Pack 1974, Hunter 1975, Goldflam 1977, Kouri 1979, Beneventi 1988) the centrifugal terms and the individual channel wavevectors which appear in the CC equations are replaced by an effective value and these equations become fully decoupled. The quantum calculation is then reduced to the resolution of a single-channel Schrödinger equation for each value of the orientation angle θ and for each value of l where l denotes in the following the average value of the orbital angular momentum of the two partners:

$$\left[\frac{d^2}{dR^2} + k^2 - \frac{l(l+1)}{R^2} - \frac{2\mu}{h} V(R,\theta) \right] C_{kl}(R,\theta) = 0, \tag{2}$$

where $V(R,\theta)$ is just the interaction potential expressed in the body frame which has been determined in Sect. 2, k is the effective value of the wavevector and l is the effective value of the orbital angular momentum. To carry out the scattering calculations, the interaction potential is expanded in the usual Legendre expansion, namely:

$$V(R,\theta) = \sum_{\lambda} V(\lambda) \, P(\cos\theta). \tag{3}$$

Since C_2 is homonuclear, only even values of λ need to be included in the expansion. In the case of C_2–He, three terms ($\lambda = 0, 2, 4$) were sufficient to reproduce the potential.

Table 2. Rotational deexcitation rate constants[a] in the C_2 $X(^1\Sigma^+)$ molecule in collisions with He and H_2

T(K)	300		500		1000	
	C_2-He	C_2-H_2	C_2-He	C_2-H_2	C_2-He	C_2-H_2
k(2->0)	2.8	1.4	3.6	1.6	4.6	2.9
k(4->2)	4.9	2.2	6.9	2.4	9.8	4.5
k(6->4)	5.2	2.8	7.4	2.9	10.7	5.2
k(8->6)	5.4	2.5	7.6	3.0	10.9	5.6
k(10->8)	5.6	3.3	7.8	3.6	11.1	6.3

[a] units are in $cm^3/s \times 10^{11}$

Asymptotically, the radial functions $C_{kl}(R, \theta)$ solutions of the Eq. (2) are subject to proper boundary conditions and are expressed in terms of angle dependent sudden functions $S_{kl}(\theta)$. The IOS S-matrix elements are then obtained as matrix elements of the angle dependent sudden functions and the degeneracy-averaged integral cross sections can be written as:

$$\sigma_{j \to j'} = \frac{\pi}{k^2} \sum_{Jll'} (2J+1) |S_{jl, j'l'}|^2, \qquad (4)$$

where $S_{jlj'l'}$ denotes the S-matrix elements.

Subsequently, the rate constants are determined by averaging $v\sigma$ over a Maxwellian distribution of the velocities v. In the IOS calculations, the angle dependent sudden functions are usually expressed in terms of phase shifts, namely

$$S_{kl}(\theta) = e^{2i\eta_l}(\theta), \qquad (5)$$

and the angle dependent phase shifts η_l are calculated for each partial wave l within the JWKB approximation by a Gauss-Mehler integration. Integral IOS cross sections are determined from the angle dependent sudden functions using the powerful factorization properties shown by Pack (1974) and Goldflam (1977). As pointed out by Fitz (1978) and by Buck & Khare (1977) degeneracy-averaged integral cross sections are virtually independent of the choice of l. The present calculations were based on the computationally efficient initial l labeling scheme.

Infinite-order-sudden calculations were carried out at several total energies ranging from $100\,cm^{-1}$ to $3500\,cm^{-1}$ and the rate constants were calculated for three temperatures $T = 300\,K$, $500\,K$ and $1000\,K$. The C_2 molecule was treated as a rigid rotor. Since the C_2 molecule is homonuclear with no nuclear spin, only rotational states with even values of j exist. Table 2 gives the calculated deexcitation rate constants for C_2 deexcitation by para H_2 calculated recently by Lavendy et al. (1991). We observe that, although the rate constants are of the same order of magnitude for the two systems, the values in C_2-He are about two times greater than the corresponding ones in the C_2-H_2 system. To comment this point, we have plotted in Fig. 2 the dependence on internuclear separation of the interaction potentials in the case of linear ($V_{//}$) and perpendicular ($V_\perp$) geometries for the C_2-He and the
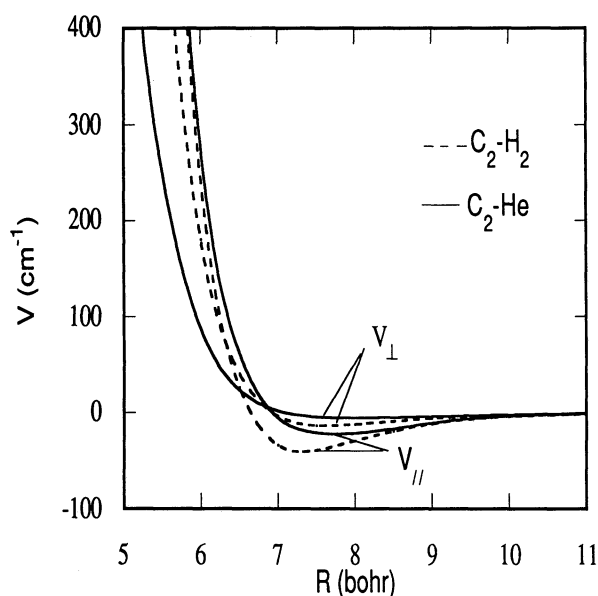
Fig. 2. Linear and perpendicular potentials for C_2–He and C_2–H_2

C_2–H_2 systems. We see clearly in this figure that the anisotropy, which can be assessed as the difference between $V_{//}$ and $V_\perp$ is, for both systems, large in the region of the repulsive walls but rather small in the long-range region. Moreover, the anisotropy in the short-range region is stronger in the case of C_2–He than in the case of C_2–H_2. Since inelastic transitions are sensitive mostly to the short-range region of the potentials in the sudden regime, we expect, and observe in Table 2, that the calculated cross sections will be larger for C_2–He than for C_2–H_2.

682

acknowledged. Computations have been performed on an IBM 3090 at Circe (Orsay, France).

References

Arthurs A., Dalgarno A., 1960, Proc. Roy. Soc. (London Ser.) A 256, 540
Beneventi L., Casavecchia P., Vecchiocattivi F., Volpi G.G., Lemoine D., Alexander M.H., 1988, J. Chem. Phys. 89, 3505
Boys S.F., Bernardi F., 1970, Mol. Phys. 19, 553
Buck U., Khare W., 1977, Chem. Phys. 26, 215
Chambaud G., Gérard-Aïn M., Kassab E., Levy B., Pernot P., 1984, Chem. Phys. 90, 271
Dickinson A.S., 1979, Comput. Phys. Comm. 17, 51
Fitz D.E., 1978, Chem. Phys. Lett. 55, 202
Goldflam R., Green S., Kouri D.J., 1977, J. Chem. Phys. 67, 4149
Goldflam R., Kouri D.J., Green S., 1977, J. Chem. Phys. 67, 5661
Hunter L.W., 1975, J. Chem. Phys. 62, 2855
Huzinaga S., 1965, J. Chem. Phys. 42, 1293
Huzinaga S., Sakai Y., 1969, J. Chem. Phys. 50, 1371
Kouri D.J., 1979, in: Atom-Molecule Collision Theory: A Guide for the Experimentalist, ed. R.B. Berstein, Plenum, New York, p. 301
Lavendy H., Robbe J.M., Chambaud G., Levy B., 1987, Chem. Phys. 116, 11
Lavendy H., Robbe J.M., Roueff E., 1991, A&A 241, 343
Lavendy H., Robbe J.M., Chambaud G., Levy B., Roueff E., 1991, A&A 251, 365
Miller S., Tennyson J., Follmeg B., Rosmus P., Werner H.J., 1988, J. Chem. Phys. 89, 2178
Pack R.T., 1974, J. Chem. Phys. 60, 633
Secrest D., 1975, J. Chem. Phys. 62, 710; see also, D. Secrest, 1979, in: Atom-Molecule Collision Theory: A Guide for the Experimentalist, ed. R.B. Berstein, Plenum, New York, p. 265
Souza S.P., Lutz B.L., 1976, ApJ 216, L49
Souza S.P., Lutz B.L., 1977, ApJ 218, L31

© European Southern Observatory • Provided by the NASA Astrophysics Data System

682

acknowledged. Computations have been performed on an IBM 3090 at Circe (Orsay, France).

References

Arthurs A., Dalgarno A., 1960, Proc. Roy. Soc. (London Ser.) A 256, 540
Beneventi L., Casavecchia P., Vecchiocattivi F., Volpi G.G., Lemoine D., Alexander M.H., 1988, J. Chem. Phys. 89, 3505
Boys S.F., Bernardi F., 1970, Mol. Phys. 19, 553
Buck U., Khare W., 1977, Chem. Phys. 26, 215
Chambaud G., Gérard-Aïn M., Kassab E., Levy B., Pernot P., 1984, Chem. Phys. 90, 271
Dickinson A.S., 1979, Comput. Phys. Comm. 17, 51
Fitz D.E., 1978, Chem. Phys. Lett. 55, 202
Goldflam R., Green S., Kouri D.J., 1977, J. Chem. Phys. 67, 4149
Goldflam R., Kouri D.J., Green S., 1977, J. Chem. Phys. 67, 5661
Hunter L.W., 1975, J. Chem. Phys. 62, 2855
Huzinaga S., 1965, J. Chem. Phys. 42, 1293
Huzinaga S., Sakai Y., 1969, J. Chem. Phys. 50, 1371
Kouri D.J., 1979, in: Atom-Molecule Collision Theory: A Guide for the Experimentalist, ed. R.B. Berstein, Plenum, New York, p. 301
Lavendy H., Robbe J.M., Chambaud G., Levy B., 1987, Chem. Phys. 116, 11
Lavendy H., Robbe J.M., Roueff E., 1991, A&A 241, 343
Lavendy H., Robbe J.M., Chambaud G., Levy B., Roueff E., 1991, A&A 251, 365
Miller S., Tennyson J., Follmeg B., Rosmus P., Werner H.J., 1988, J. Chem. Phys. 89, 2178
Pack R.T., 1974, J. Chem. Phys. 60, 633
Secrest D., 1975, J. Chem. Phys. 62, 710; see also, D. Secrest, 1979, in: Atom-Molecule Collision Theory: A Guide for the Experimentalist, ed. R.B. Berstein, Plenum, New York, p. 265
Souza S.P., Lutz B.L., 1976, ApJ 216, L49
Souza S.P., Lutz B.L., 1977, ApJ 218, L31

© European Southern Observatory • Provided by the NASA Astrophysics Data System